

1N-20  
63132  
p37

# Development of a Single-Phase Harmonic Power Flow Program to Study the 20 kHz A.C. Power System for Large Spacecraft

L. Alan Kraft  
*Valparaiso University*  
*Valparaiso, Indiana*

and

M. David Kankam  
*Lewis Research Center*  
*Cleveland, Ohio*

November 1991



(NASA-TM-105326) DEVELOPMENT OF A  
SINGLE-PHASE HARMONIC POWER FLOW PROGRAM TO  
STUDY THE 20 KHZ AC POWER SYSTEM FOR LARGE  
SPACECRAFT (NASA) 37 5 CSCL 105

N92-13275

Unclass  
G3/20 0053182



## **TABLE OF CONTENTS**

NOMENCLATURE.....	iii
<b><u>Abstract</u></b> .....	1
1. <b><u>Introduction</u></b> .....	1
2. <b><u>Operation of the Mapham Inverter</u></b> .....	3
3. <b><u>Modelling the Mapham Inverter</u></b> .....	4
4. <b><u>Operation of the Single Phase. Voltage Controlled Rectifier</u></b> .....	11
5. <b><u>Modelling the Single Phase. Voltage Controlled Rectifier</u></b> .....	12
6. <b><u>The Harmonic Power Flow Algorithm</u></b> .....	17
7. <b><u>Modifying the Harmonic Power Flow Algorithm</u></b> .....	21
8. <b><u>Examples</u></b> .....	24
9. <b><u>Conclusions and Recommendations</u></b> .....	27
LIST OF REFERENCES.....	29
Appendix A.....	30



## NOMENCLATURE

$a$	Coefficient of a polynomial
AC	Alternating current
$[A]$	Matrix A
$[A]^T$	Transpose of matrix A
$[A^{(i)}]$	Matrix A at the $i^{\text{th}}$ iteration
$A^{(i)}$	The $i^{\text{th}}$ harmonic component of A
$\Delta A$	The change in A
$\alpha$	Real component of a complex frequency
$b$	Coefficient of a polynomial
$c$	Real component of a complex Fourier coefficient
C	Capacitance
$d$	Imaginary component of a complex Fourier coefficient
D	Magnitude of a complex Fourier Coefficient
D'	Normalized value of D
DC	Direct current
$f$	Frequency
GDC	General Dynamics Corporation
I	Current magnitude
I(s)	Current in the frequency domain
Im[A]	Imaginary component of A
$j$	$(-1)^{0.5}$
$[J]$	Jacobian matrix
$[J_{ij}]$	$i,j$ element of the Jacobian matrix
L	Inductance

$\lambda$	Substitute for $\{[4/(LC) - (1/RC)^2]^{0.5}\}/2$
K	Magnitude of a coefficient of a partial fraction
K	Complex coefficient of a partial fraction
$\omega$	Imaginary component of a complex frequency
P	Poles of a circuit
	Real power
Q	Reactive volt-ampere
R	Resistance
Re[A]	Real component of A
s	Complex frequency
SCR	Silicon controlled rectifier
$\sigma$	Substitute for $1/(2RC)$
THD	Total harmonic distortion
$\tau$	Time constant
	Period of a sinusoidal waveform
$\theta$	Angle of a complex Fourier coefficient
	Angle of a coefficient of a partial fraction
V	Voltage magnitude
V	Voltage in the frequency domain
X	Reactance
Z	Complex impedance

# **Development of a Single-Phase Harmonic Power Flow Program to Study the 20 kHz AC Power System for Large Spacecraft**

**L. Alan Kraft\***  
Valparaiso University  
Valparaiso, Indiana 46383

and

**M. David Kankam**  
National Aeronautics and  
Space Administration  
Lewis Research Center  
Cleveland, Ohio 44135

## **Abstract**

This report describes the development of a software to aid in the design and analysis of AC power systems for large spacecraft. The algorithm is an improved version of Electric Power Research Institute's (EPRI) harmonic power flow program, "HARMFLO", used for the study of AC power quality. The new program is applicable to three-phase systems typified by terrestrial power systems, and single-phase systems characteristic of space power systems. The modified "HARMFLO" accommodates system operating frequencies ranging from terrestrial 60 hz to and beyond aerospace 20 kHz, and can handle both source and load-end harmonic distortions.

Comparison of simulation and test results of a representative spacecraft power system shows a satisfactory correlation. Recommendations are made for the direction of future improvements to the software, to enhance its usefulness to power system designers and analysts.

## **Introduction**

The advent of large spacecraft has resulted in their increased electrical energy consumption. Additionally, planned space exploration will require more capability for extended human and equipment support. These requirements are well served by the AC power system. However, the presence of switching devices in the converters at the source end of currently proposed, spacecraft AC system and their connected nonlinear loads can cause several problems in the power system. One of the more serious problems is the occurrence of harmonic resonance. This is a phenomenon whereby the harmonics generated by the switching devices and the nonlinear loads excite resonant modes caused by cancellation or near cancellation of inductive reactance by capacitive reactance.

---

\*1990 NASA/ASEE Summer Faculty Fellow at Lewis Research Center.

Among the problems caused by voltage and current resonance in a power system are insulation failure due to overvoltage, equipment malfunction resulting from high frequency and multiple zero-crossings of distorted waveforms, radio-frequency noise, and transmission and equipment current overloads. Generally, the generated harmonics tend to worsen the overall power quality.

This report describes a harmonic power flow program, "HARMFLO," for identifying and evaluating resonance problems, among others, which can occur in either terrestrial or large spacecraft power systems. The program accepts both three-phase systems commonly found in terrestrial power systems, and single-phase systems characteristic of spacecraft power systems. The applicability of the program encompasses frequencies ranging from terrestrial 60 Hz to aerospace 20 kHz and beyond, and harmonic distortion at the source - and load-ends of the power system.

In its present phase, the harmonic power flow program contains a mathematical model of a Mapham inverter [1], a key subsystem of a representative 20 kHz spacecraft power system used in developing and testing the algorithm. In consideration of criticality of payload weight, the salient features of lightweight and simple design, with a minimum number of components, make the Mapham inverter an attractive source of AC power for spacecraft applications. Inclusion of the inverter model in the algorithm can expedite required performance analysis of the spacecraft power systems during their design phase. The design and operation of the Mapham inverter is well documented in the literature [1-3]. Hence, only the particular aspects of the inverter operation which impacts its modelling are discussed in this report.

Another essential subsystem of the representative power system used is the single-phase voltage controlled rectifier. As a potential source of harmonic current with attendant problems in the power system, the mathematical model for this rectifier is also developed.

Simulated preliminary results obtained from the algorithm compare favorably with published test results. Recommendations included in the report point to future enhancements to the power flow program to make it more useful to power system designers and analysts.



## 2. Operation of the Mapham Inverter

The circuit diagram of a Mapham inverter is shown in Figure 1. The SCR's are switched at the desired output frequency,  $f_s$ . This switching reverses the current through the capacitor,  $C_r$ . This current resonates at a frequency determined by the series combination of the inductor,  $L_r$ , and  $C_r$ . The reversing of the current at a time when the resonating current is in its negative half cycle will sustain the inverter's operation as an AC source. Figures 2 through 4, which can be found in the publication by Sundberg, Brush, Button and Patterson [3], show the reversing currents,  $I_{L1}$  and  $I_{L2}$ , through the inductors,  $L_r/2$ , and the total resulting current through  $C_r$ . It is important to note that unless the resonant frequency,  $f_r$ , is the same as  $f_s$ , a distortion occurs in the capacitor current waveform. This distortion results in harmonic currents which are injected into the power system by the inverter. Since the impedance of the load placed across the output terminals of the inverter will change  $f_r$ , loading will affect the level of injected harmonic current.

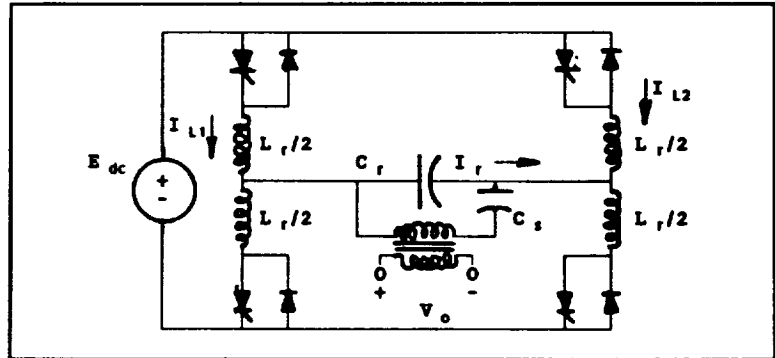


Figure 1 - Circuit Diagram of a Mapham Inverter.

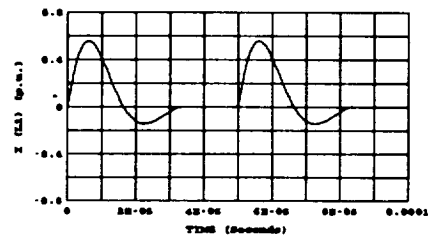


Figure 2 - Current  $I_{L1}$ .

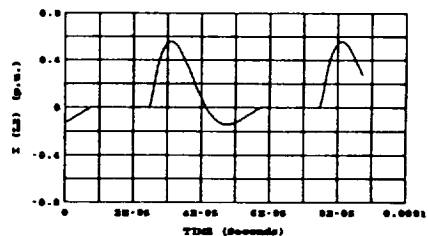


Figure 3 - Current  $I_{L2}$ .

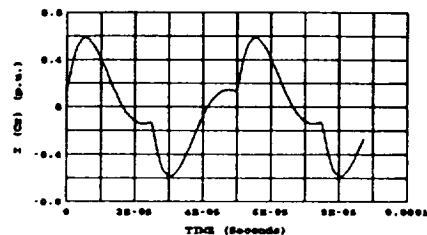


Figure 4 - Total Current Through Capacitor  $C_r$ .

### 3. Modelling the Mapham Inverter

To determine the injection currents that will occur for a certain power system configuration, it is necessary to find  $f_r$  for the inverter under the desired loading. Under no-load conditions, the resonant frequency is given by

$$f_r = \frac{1}{2\pi\sqrt{LC}} .$$

When the inverter is connected to the power system, the system appears as an equivalent impedance of  $Z_{eq} = R_{eq} + jX_{eq}$  connected across the output terminals of the inverter as shown in Figure 5. In the frequency domain, the input current resulting from a step input voltage has the form

$$\frac{a_m s^m + \dots + a_1 s + a_0}{b_n s^n + \dots + b_1 s + b_0}$$

where,  $m < n$  and the coefficients of the two polynomials depend on whether the system equivalent is capacitive or inductive (i.e.,

whether  $Z_{eq} = R_{eq} - jX_{eq}$  or  $Z_{eq} = R_{eq} + jX_{eq}$ ). The details concerning the derivation of these polynomials can be found in Appendix A.

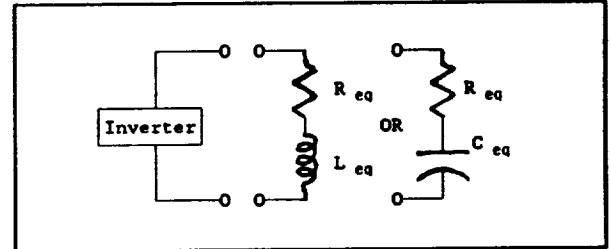


Figure 5 - Power System Equivalent.

If the system equivalent is inductive then  $n = 5$ , and the coefficients of the denominator are:

$$b_5 = (L_1 + L_{eq}) L_r C_r C_s ,$$

$$b_4 = R_{eq} L_r C_r C_s ,$$

$$b_3 = (L_1 + L_{eq}) C_s + \left( 1 + \frac{L_1 + L_{eq}}{L_m} \right) L_r (C_r + C_s) ,$$

$$b_2 = R_{eq} C_s + \frac{R_{eq} L_r (C_s + C_r)}{L_m} ,$$

$$b_1 = 1 + \frac{L_1 + L_{eq}}{L_m} , \text{ and}$$

$$b_0 = \frac{R_{eq}}{L_m} .$$

However, if the equivalent is capacitive then  $n = 6$ , and the coefficients of the denominator are:

$$b_6 = L_1 L_r C_{eq} C_r C_s ,$$

$$b_5 = R_{eq} L_r C_{eq} C_r C_s ,$$

$$b_4 = L_1 C_{eq} C_s + L_r C_r C_s + L_r C_{eq} C_r + L_r C_{eq} C_s + \frac{L_1 L_r C_{eq} (C_r + C_{eq})}{L_m} ,$$

$$b_3 = R_{eq} C_{eq} C_s + \frac{R_{eq} L_r C_{eq} (C_s + C_r)}{L_m} ,$$

$$b_2 = C_{eq} + C_s + \frac{L_r (C_{eq} + C_r)}{L_m} ,$$

$$b_1 = \frac{R_{eq} C_{eq}}{L_m} , \text{ and}$$

$$b_0 = \frac{1}{L_m} .$$

Once the coefficients are computed, the denominator can then be factored into

$$(s_n + P_n) (s_{n-1} + P_{n-1}) \dots (s_2 + P_2) (s_1 + P_1) .$$

The roots of this polynomial (i.e., the P's) represent the poles of the network. Since the network is primarily a series L-C circuit, at least two of the poles will form a complex pair with the form:

$$(s_r + \alpha_r + j\omega_r) (s_{r-1} + \alpha_r - j\omega_r) .$$

Since  $n > m$ , this polynomial is said to be a proper rational polynomial and can be expressed in partial fraction form:

$$\frac{K_n}{s_n + P_n} + \dots + \frac{K_r}{s_r + \alpha_r - j\omega_r} + \frac{K_r^*}{s_r + \alpha_r + j\omega_r} + \dots + \frac{K_1}{s_1 + P_1} .$$

The function can then be returned to the time domain by using inverse Laplace transforms. The inverse transform for the complex pair is

$$\mathcal{L}^{-1}\left[\frac{K\angle\theta}{s+\alpha-j\beta} + \frac{K\angle-\theta}{s+\alpha+j\beta}\right] = 2Ke^{-\alpha t}\cos(\beta t+\theta) . \quad (1)$$

This yields a time domain response for the current through  $C_r$ , which is

$$I_{C_r}(t) = I_o e^{-\alpha_r t} \sin(\omega_r t + \theta_r) + \begin{matrix} \text{responses due} \\ \text{to the other} \\ \text{poles} \end{matrix} .$$

Once the natural resonate frequency and its corresponding period

$$\tau_r = \frac{1}{f_r} = \frac{2\pi}{\omega_r}$$

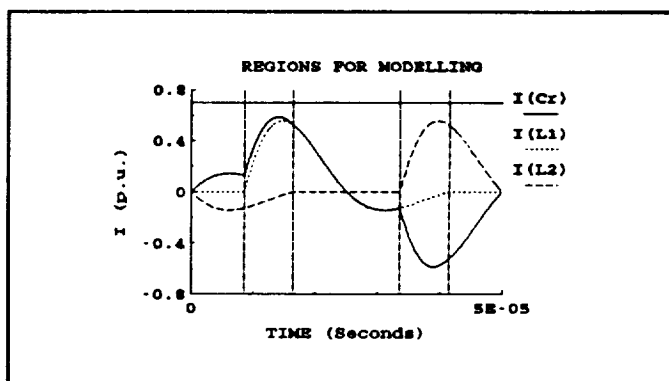


Figure 6 - Capacitor Current,  $C_r$ ; Inductor Currents,  $I_{L1}$  and  $I_{L2}$  with Indicated Regions for Modelling.

are known, the components of the generated harmonic currents can be determined. Figure 6 shows one period of the current through  $C_r$ . Also shown in Figure 6 are the corresponding currents  $I_{L1}$  and  $I_{L2}$  which flow through each set of switched inductors. From this information, the capacitor current can be written as a function of time over five individual regions of the waveform. The resulting equations are:

$$I_{C_r}(t) = -e^{-\alpha(t+\frac{\tau_r}{2})} \sin(\omega_r t + \pi) \quad (2)$$

for  $0 \leq t < \frac{\tau_s - \tau_r}{2}$  ,

$$I_{C_r}(t) = e^{-\alpha(t-\frac{\tau_s - \tau_r}{2})} \sin\left[\omega_r t - \pi\left(\frac{\tau_s - \tau_r}{\tau_r}\right)\right] - e^{-\alpha(t+\frac{\tau_r}{2})} \sin(\omega_r t + \pi) \quad (3)$$

for  $\frac{\tau_s - \tau_r}{2} \leq t < \frac{\tau_r}{2}$  ,

$$I_{C_r}(t) = e^{-\alpha(t-\frac{\tau_s - \tau_r}{2})} \sin\left[\omega_r t - \pi\left(\frac{\tau_s - \tau_r}{\tau_r}\right)\right] \quad (4)$$

for  $\frac{\tau_r}{2} \leq t < \tau_s - \frac{\tau_r}{2}$  ,

$$I_{C_r}(t) = e^{-\alpha(t-\frac{\tau_s - \tau_r}{2})} \sin\left[\omega_r t - \pi\left(\frac{\tau_s - \tau_r}{\tau_r}\right)\right] - e^{-\alpha(t-\tau_s+\frac{\tau_r}{2})} \sin\left[\omega_r t - \pi\left(\frac{2\tau_s - \tau_r}{\tau_r}\right)\right] \quad (5)$$

for  $\tau_s - \frac{\tau_r}{2} \leq t < \frac{\tau_s + \tau_r}{2}$  , and

$$I_{C_r}(t) = -e^{-\alpha(t-\tau_s+\frac{\tau_r}{2})} \sin\left[\omega_r t - \pi\left(\frac{2\tau_s - \tau_r}{\tau_r}\right)\right] \quad (6)$$

for  $\frac{\tau_s + \tau_r}{2} \leq t < \tau_s$  .

Since the current is now mathematically represented as a continuous, repetitive time function, it can be represented by a Fourier series. The Fourier series of a repetitive time function is given by

$$f(t) = c_0 + \sum_{n=1}^{\infty} c_n \cos n\omega_0 t + d_n \sin n\omega_0 t$$

where,

$$c_0 = \frac{1}{\tau_0} \int_{t_1}^{t_1 + \tau_0} f(t) dt , \quad (7)$$

$$c_n = \frac{2}{\tau_0} \int_{t_1}^{t_1 + \tau_0} f(t) \cos(n\omega_0 t) dt , \quad (8)$$

and

$$d_n = \frac{2}{\tau_0} \int_{t_1}^{t_1 + \tau_0} f(t) \sin(n\omega_0 t) dt . \quad (9)$$

The Fourier coefficients,  $c_n$  and  $d_n$ , are found by integrating Equations (2) through (6) over one period of the waveform. It should be noted that the magnitude of the current is assumed to be 1.0 at this point. Once the coefficients are computed, they are then normalized by

$$D'_i \angle \theta'_i = \frac{D_i}{D_1} \angle \theta_i - n\theta_1 . \quad (10)$$

The coefficients are normalized because the magnitude of the current will not be known until a fundamental power flow is found. The required values of  $D_1$  and  $\theta_1$  are then known.

To apply these coefficients to the harmonic power flow algorithm, it is first necessary to understand the formulation of the harmonic power flow algorithm itself. The details of how this will be done are covered in Section 7 of this report.



#### 4. Operation of the Single Phase, Voltage Controlled Rectifier

The circuit diagram of a single phase, voltage controlled rectifier is shown in Figure 7. Since the D.C. output voltage of the rectifier is the average of the "ripple" output voltage,  $V_x$ ,

shown in Figure 8, it can be controlled by changing the firing angle,  $\alpha$ .

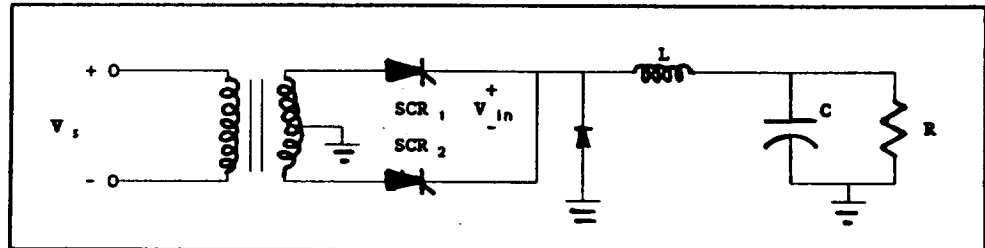


Figure 7 - Single Phase, Voltage Controlled Rectifier Circuit.

This means that,

by adjusting  $\alpha$ , the average value of the "ripple" or the D.C. output voltage can be controlled within certain limits. The SCR's are triggered with a signal which is set by  $\alpha$ . The value of  $\alpha$  is determined by the difference between the desired D.C. output voltage and the actual D.C. output voltage. Once either of the SCR's is triggered, it will conduct until the voltage on the anode is less than the voltage on the cathode. This occurs when the input voltage,  $V_{in}$ , drops below the output voltage,  $V_{out}$ , at  $\beta$ , the commutation angle.

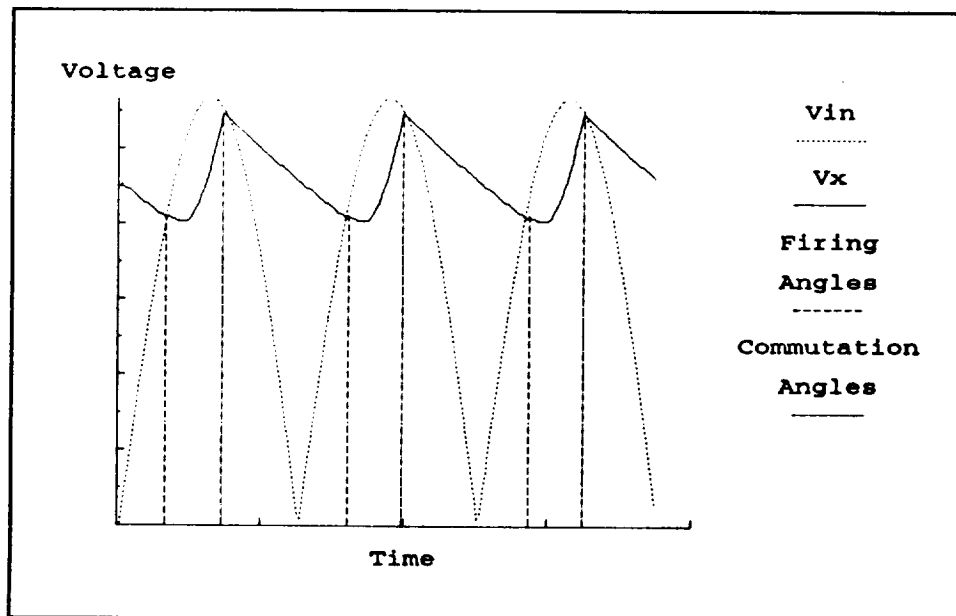


Figure 8 - Input Voltage to a Single Phase, Voltage Controlled Rectifier Circuit.

## 5. Modelling the Single Phase, Voltage Controlled Rectifier

When either of the SCR's is triggered, the voltage which is applied to the input terminals of the rectifier is given by

$$V_{in}(t) = V_m \sin(\omega_s t + \alpha) u(t) .$$

This function becomes the following in the frequency domain:

$$V_{in}(s) = V_m \left[ \frac{s \sin \alpha + \omega_s \cos \alpha}{s^2 + \omega_s^2} \right] . \quad (11)$$

The entire single phase rectifier circuit in the frequency domain is shown in Figure 9. The current source,  $CV(0^+)$ , is needed to account for any initial voltage that might be present on the capacitor when the SCR is fired at  $\alpha$ . Since  $I_{in}(s)$  is given by

$$I_{in}(s) = \frac{V_{in}(s) - V_x(s)}{sL} , \quad (12)$$

$V_x(s)$  must be determined. This is done by writing Kirchhoff's current law at the node with the unknown voltage,  $V_x(s)$ .

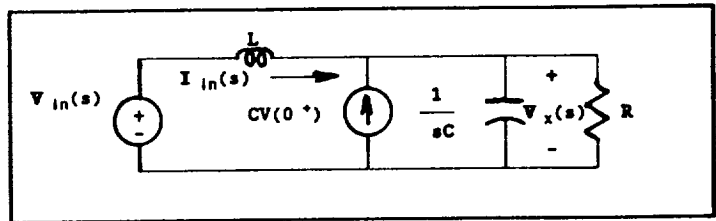


Figure 9 - Single Phase, Voltage Controlled Rectifier Circuit in the Frequency Domain.

The result is

$$\begin{aligned}
 sCV_x(s) + \frac{V_x(s)}{R} &= \frac{\frac{V_m (s \sin \alpha + \omega_s \cos \alpha)}{(s^2 + \omega_s^2)} - V_x(s)}{sL} + CV(0^+) \\
 V_x(s) \left( sC + \frac{1}{R} + \frac{1}{sL} \right) &= \frac{V_m (s \sin \alpha + \omega_s \cos \alpha) + sLC (s^2 + \omega_s^2) V(0^+)}{sL (s^2 + \omega_s^2)} \quad (13) \\
 V_x(s) &= \frac{\frac{1}{LC} [V_m (s \sin \alpha + \omega_s \cos \alpha) + sLC (s^2 + \omega_s^2) V(0^+)]}{\left( s^2 + \frac{s}{RC} + \frac{1}{LC} \right) (s^2 + \omega_s^2)} .
 \end{aligned}$$

If Equations (11) and (13) are substituted into Equation (12), the result is

$$\begin{aligned}
 I_{Lm}(s) &= \frac{\frac{V_m (s \sin \alpha + \omega_s \cos \alpha)}{(s^2 + \omega_s^2)} - \frac{\frac{1}{LC} [V_m (s \sin \alpha + \omega_s \cos \alpha) + sLC (s^2 + \omega_s^2) V(0^+)]}{\left( s^2 + \frac{s}{RC} + \frac{1}{LC} \right) (s^2 + \omega_s^2)}}{sL} \\
 &= \frac{s \left( s + \frac{1}{RC} \right) [V_m (s \sin \alpha + \omega_s \cos \alpha)] - s (s^2 + \omega_s^2) V(0^+)}{sL \left( s^2 + \frac{s}{RC} + \frac{1}{LC} \right) (s^2 + \omega_s^2)} \\
 &= \frac{\frac{V_m}{L} \left( s + \frac{1}{RC} \right) [s \sin \alpha + \omega_s \cos \alpha] - (s^2 + \omega_s^2) V(0^+)}{\left( s^2 + \frac{s}{RC} + \frac{1}{LC} \right) (s^2 + \omega_s^2)} .
 \end{aligned}$$

This can now be expressed in partial fraction form:

$$I_{in}(s) = \frac{K_1 \angle \theta_1}{s + \frac{1}{2RC} - j \frac{\sqrt{\frac{4}{LC} - \left(\frac{1}{RC}\right)^2}}{2}} + \frac{K_1 \angle -\theta_1}{s + \frac{1}{2RC} + j \frac{\sqrt{\frac{4}{LC} - \left(\frac{1}{RC}\right)^2}}{2}} + \frac{K_2 \angle \theta_2}{s - j\omega_s} + \frac{K_2 \angle -\theta_2}{s + j\omega_s}$$

where,

$$K_1 \angle \theta_1 = \left[ s + \frac{1}{2RC} - j \frac{\sqrt{\frac{4}{LC} - \left(\frac{1}{RC}\right)^2}}{2} \right] I_{in}(s) \Big|_{s = -\frac{1}{2RC} + j \frac{\sqrt{\frac{4}{LC} - \left(\frac{1}{RC}\right)^2}}{2}}$$

and

$$K_2 \angle \theta_2 = [s - j\omega_s] I_{in}(s) \Big|_{s = j\omega_s}.$$

To simplify the notation, let

$$\sigma = \frac{1}{2RC} \quad \text{and} \quad \lambda = \frac{\sqrt{\frac{4}{LC} - \left(\frac{1}{RC}\right)^2}}{2},$$

then

$$K_1 \angle \theta_1 = [s + \sigma - j\lambda] I_{Lm}(s) \big|_{s = -\sigma + j\lambda}$$

$$= \frac{\left(\frac{V_m}{L}\right)(-\sigma + j\lambda + 2\sigma)[(-\sigma + j\lambda)\sin\alpha + \omega_s \cos\alpha] - [(-\sigma + j\lambda)^2 + \omega_s^2] V(0^+)}{(j2\lambda)[(-\sigma + j\lambda)^2 + \omega_s^2]}$$

$$= \frac{\left(\frac{V_m}{L}\right)(\sigma + j\lambda)[(\omega_s \cos\alpha - \sigma \sin\alpha) + j\lambda \sin 2\alpha] - [(\sigma^2 + \lambda^2 + \omega_s^2) - j2\sigma\lambda] V(0^+)}{(j2\lambda)[(\sigma^2 + \lambda^2 + \omega_s^2) - j2\sigma\lambda]}$$

$$= \frac{\left(\frac{V_m}{L}\right)(\sigma + j\lambda)[(\omega_s \cos\alpha - \sigma \sin\alpha) + j\lambda \sin\alpha]}{(j2\lambda)[(\sigma^2 + \lambda^2 + \omega_s^2) - j2\sigma\lambda]} - \frac{V(0^+)}{j2\lambda}$$

and

$$K_2 \angle \theta_2 = [s - j\omega_s] I_{Lm}(s) \big|_{s = j\omega_s}$$

$$= \frac{\left(\frac{V_m}{L}\right)\left(j\omega_s + \frac{1}{RC}\right)(j\omega_s \sin\alpha + \omega_s \cos\alpha) - (-\omega_s^2 + \omega_s^2) V(0^+)}{\left(-\omega_s^2 + j\frac{\omega_s}{RC} + \frac{1}{LC}\right)(j2\omega_s)}$$

$$= \frac{\left(\frac{V_m}{L}\right)\left(\frac{1}{RC} + j\omega_s\right)(\omega_s \angle \alpha) - (0) V(0^+)}{\left[\left(\frac{1}{LC} - \omega_s^2\right) + j\frac{\omega_s}{RC}\right](j2\omega_s)}$$

$$= \frac{\left(\frac{V_m}{2L}\right)\left(\frac{1}{RC} + j\omega_s\right)\left[\cos\left(\alpha - \frac{\pi}{2}\right) + j\sin\left(\alpha - \frac{\pi}{2}\right)\right]}{\left[\left(\frac{1}{LC} - \omega_s^2\right) + j\frac{\omega_s}{RC}\right]}$$

Once the complex coefficients,  $K_1$  and  $K_2$ , are computed, the transformation back into the time domain is found using Equation (1). Now that the input current is known in the time domain, Equations (7), (8), and (9) can be used to find the Fourier coefficients of the current. It is important to note that, because the total current is known at this point, normalization of the rectifier coefficients is not needed.

These coefficients, like those found for the Mapham inverter, must be incorporated into the harmonic power flow program. To accomplish these goals, the following is a brief summary of the development of the harmonic power flow program.

## 6. The Harmonic Power Flow Algorithm

The harmonic power flow algorithm used in this work is the one developed by Heydt and Xia [4,5] and later modified by Grady [6]. The algorithm uses a standard Newton-Raphson formulation for a power flow program. The basic algorithm is:

1. Select an initial solution vector for all bus voltages,  $[V^{(0)}]$ , where element  $j$  is  $|V_j|$  and  $\theta_j$  or the complex voltage at bus  $j$ .
2. Using the voltage vector, calculate

$$\Delta P_j = P_j^{scheduled} - P_j^{calculated}$$

$$\Delta Q_j = Q_j^{scheduled} - Q_j^{calculated} .$$

If  $\Delta P$  and  $\Delta Q$  for all busses are  $\leq \epsilon$ , a specified tolerance, a solution has been reached; and, the iterative process is stopped; and, the output is printed.

3. Compute the elements of the Jacobian matrix which are defined by

$$[J_{ij}] = \begin{bmatrix} \frac{\partial P_i}{\partial V_j} & \frac{\partial P_i}{V_j \partial \delta_j} \\ \frac{\partial Q_i}{\partial V_j} & \frac{\partial Q_i}{V_j \partial \delta_j} \end{bmatrix} .$$

4. Using  $[\Delta P, \Delta Q]^T = [J][\Delta V, \Delta \delta]^T$ , calculate  $\Delta V$  and  $\Delta \delta$ .
5. Update the solution voltage vector,

$$[V^{(l)}] = [V^{(l-1)}] + [\Delta V, \Delta \delta]^T.$$

6. Repeat Steps 2 through 5.

This basic power flow algorithm was modified by Heydt, Xia and Grady in the following manner.

1. The basic algorithm described above is run on the system for the fundamental frequency only.
2. The solution voltage vector obtained in Step 1 is used as the initial value in the harmonic power flow. Therefore, the initial voltage vector is

$$\begin{bmatrix} V^{(1)} \\ V^{(2)} \\ V^{(3)} \\ \vdots \\ V^{(n)} \\ \Phi \end{bmatrix}$$

where,  $V^{(i)}$  represents the bus voltage for the  $i^{\text{th}}$  harmonic and  $\Phi$  are the firing and commutation angles for the converters.



3. Using the solution vector, calculate

$$\Delta P_j = P_j^{\text{scheduled}} - P_j^{\text{calculated}}$$

$$\Delta Q_j = Q_j^{\text{scheduled}} - Q_j^{\text{calculated}}$$

$$\Delta I^{(i)} = I^{(i)} \text{ scheduled} - I^{(i)} \text{ calculated} \quad (14)$$

where,  $I^{(i)} \text{ scheduled}$  is the scheduled  $i^{\text{th}}$  harmonic current at each bus, and  $I^{(i)} \text{ calculated}$  is the calculated  $i^{\text{th}}$  harmonic current at each bus. It should be noted that the scheduled current for all busses except harmonic source (i.e., nonlinear devices) is 0. If  $\Delta P$ ,  $\Delta Q$ , and  $\Delta I$  are  $< \epsilon$ , a specified tolerance, for all busses, the solution has been reached; and, the algorithm is finished.

4. Calculate the elements of the modified Jacobian matrix. The Jacobian matrix is modified by formatting it as follows

$$[J] = \begin{bmatrix} J^{(1)} & J^{(2)} & \dots & J^{(n)} & 0 \\ TG^{(2,1)} & TG^{(2,2)} & \dots & TG^{(2,h)} & H^{(2)} \\ \cdot & \cdot & \dots & \cdot & \cdot \\ TG^{(h,1)} & TG^{(h,2)} & \dots & TG^{(h,h)} & H^{(h)} \\ TG^{(1,1)} & TG^{(1,1)} & \dots & TG^{(1,h)} & H^{(1)} \end{bmatrix}$$

where,

$$J_{ij}^{(m)} = \begin{bmatrix} \frac{\partial P_j^{(m)}}{\partial V_j^{(m)}} & \frac{\partial P_j^{(m)}}{V_j \partial \delta_j^{(m)}} \\ \frac{\partial Q_j^{(m)}}{\partial V_j^{(m)}} & \frac{\partial Q_j^{(m)}}{V_j \partial \delta_j^{(m)}} \end{bmatrix}$$

$$TG_{ij}^{(m,n)} = \begin{bmatrix} \frac{\partial \text{Re}(I_j^{(m)})}{\partial V_j^{(n)}} & \frac{\partial \text{Re}(I_j^{(m)})}{\partial \delta_j^{(n)}} \\ \frac{\partial \text{Im}(I_j^{(m)})}{\partial V_j^{(n)}} & \frac{\partial \text{Im}(I_j^{(m)})}{\partial \delta_j^{(n)}} \end{bmatrix}$$

and

$$H_{ij}^{(m)} = \begin{bmatrix} \frac{\partial \text{Re}(I_j^{(m)})}{\partial \alpha_j} & \frac{\partial \text{Re}(I_j^{(m)})}{\partial \beta_j} \\ \frac{\partial \text{Im}(I_j^{(m)})}{\partial \alpha_j} & \frac{\partial \text{Im}(I_j^{(m)})}{\partial \beta_j} \end{bmatrix}$$

5. Using  $[\Delta P, \Delta Q, \Delta I]^T = [J] [\Delta V, \Delta \delta, \Delta \alpha, \Delta \beta]^T$ , calculate  $\Delta V, \Delta \delta, \Delta \alpha, \Delta \beta$ .

6. Update

$$[V^{(i)}, \delta^{(i)}, \alpha^{(i)}, \beta^{(i)}]^T = [V^{(i-1)}, \delta^{(i-1)}, \alpha^{(i-1)}, \beta^{(i-1)}]^T + [\Delta V, \Delta \delta, \Delta \alpha, \Delta \beta]^T.$$

7. Repeat Steps 3 through 6.

The modifications introduced in the basic power flow make the HARMFLO different from others which use the fundamental power and harmonic current responses of the nonlinear devices to solve the voltage levels within a power system [7]. Furthermore, the HARMFLO differs from the Alternate Transients Program (ATP) version of the Electromagnetic Transient Program (EMTP) [8]. The ATP version is used in analysis in which the nonlinear loads are represented by harmonic current injections at desired nodes within the power system.

## 7. Modifying the Harmonic Power Flow Algorithm

Since three phase, synchronous machines used in terrestrial power systems are designed to produce an undistorted 60 Hz sine wave under normal operating conditions, these electric power producing machines do not inject harmonic currents into the power grid. Because of this fact, the harmonic power flow program described above does not include the ability of the electric power sources to inject harmonic currents into the electrical system. Inverters, particularly the Mapham inverter, are, however, large producers of harmonic injection currents. These inverters inject the harmonic current at the bus where they are connected to the system. This change in sources required a modification to the harmonic power flow program.

As previously stated, the Fourier coefficients of the capacitor current,  $I_{cr}$ , are computed by inserting Equations (2) through (6) into Equations (7) through (9) and integrating over the appropriate ranges. The resulting complex coefficients are then normalized by Equation (10). This process is summarized by

$$\begin{aligned} I_j(t) &= \operatorname{Re} \left[ \sum_{n=1}^{\infty} (D_j^{(n)} \angle \theta_j^{(n)}) e^{jn\omega_0 t} \right] \\ &= \operatorname{Re} (D_j^{(1)} \angle \theta_j^{(1)} e^{j\omega_0 t} + D_j^{(2)} \angle \theta_j^{(2)} e^{j2\omega_0 t} + \dots) \\ I_j(t)^{\text{normalized}} &= \operatorname{Re} (1 \angle 0^\circ e^{j\omega_0 t} + \left( \frac{D_j^{(2)}}{D_j^{(1)}} \right) \angle (\theta_j^{(2)} - \theta_j^{(1)}) e^{j2\omega_0 t} + \dots) \\ &= \operatorname{Re} (1 \angle 0^\circ e^{j\omega_0 t} + D_j^{(2)'} \angle \theta_2' e^{j2\omega_0 t} + \dots) . \end{aligned}$$

Therefore, the magnitudes of the actual injection currents at every inverter bus for each harmonic can be determined by multiplying the magnitude of the fundamental source current at the bus by the appropriate Fourier coefficient. Thus, the scheduled injection current for an inverter bus  $j$  during the solution of the harmonic power flow can be

determined as follows by using the fundamental current magnitude and angle,  $I_j^{(1)}$  and  $\psi_j^{(1)}$ , which is found in Step 3 of the modified algorithm described in Section 6:

$$\begin{aligned}
 I_j(t)^{scheduled} &= (I_j^{(1)} \angle \psi_j^{(1)}) (I_j(t)^{normalized}) \\
 &= (I_j^{(1)} \angle \psi_j^{(1)}) [Re(1 \angle 0^\circ e^{j\omega_0 t} + D_j^{(2)'} \angle \theta_j^{(2)'} e^{j2\omega_0 t} + \dots) \\
 &= Re[I_j^{(1)} \angle \psi_j^{(1)} e^{j\omega_0 t} + I_j^{(1)} (D_j^{(2)'}) \angle (\theta_j^{(2)'} + n\psi_j^{(1)}) e^{j\omega_0 t} \\
 &= Re[I_j^{(1)} \angle \psi_j^{(1)} e^{j\omega_0 t} + I_j^{(2)} \angle \psi_j^{(2)} e^{j2\omega_0 t} + \dots] .
 \end{aligned}$$

The injected harmonic currents are then placed in the appropriate locations in Equation (14). In order to place the harmonic injection currents into Equation (14), it is necessary to represent them in rectangular form (i.e.,  $X + jY$ ). Therefore, the current at each harmonic is found by

$$\begin{aligned}
 I_{j, Re}^{(m) scheduled} &= I_j^{(m)} \cos(\psi_j^{(m)}) \\
 &= (I_j^{(1)}) (D_j^{(m)'}) \cos(\theta_j^{(m)'} - n\theta_j^{(1)}) \\
 &= (I_j^{(1)}) (\sqrt{c_j^{(m)'^2} + d_j^{(m)'^2}}) \cos\left[\tan^{-1}\left(\frac{d_j^{(m)'}}{c_j^{(m)'}}\right) - n\theta_j^{(1)}\right]
 \end{aligned}$$

and, in a similar manner,

$$I_{j, Im}^{(m) scheduled} = (I_j^{(1)}) (\sqrt{c_j^{(m)'^2} - d_j^{(m)'^2}}) \sin\left[\tan^{-1}\left(\frac{d_j^{(m)'}}{c_j^{(m)'}}\right) - n\theta_j^{(1)}\right] .$$

The harmonic power flow program does model nonlinear devices such as rectifiers. The problem is that these rectifiers are three phase. Three phase rectifiers do not mathematically function like a single phase rectifier. For this reason, modifications in the harmonic power flow code are necessary. The modifications needed to successfully incorporate single phase rectifiers into the harmonic power flow code are simply to place the various harmonic injection currents described in Section 5 of this report into the scheduled current vector:

$$I_{j, Re}^{(m) \text{ scheduled}} = c_m \quad \text{and} \quad I_{j, Im}^{(m) \text{ scheduled}} = d_m .$$

Once this is done for all Mapham inverters and single phase rectifiers, the harmonic power flow program is allowed to proceed per the algorithm described in Section 4.

## 8. Examples

To demonstrate the practicality of the theories presented in this report, the following examples are offered. The first example will investigate the voltage distortion experienced in the power system depicted in Figure 10. This example is drawn from data obtained from the

General Dynamics Corporation (GDC) 20 kHz Testbed which was developed to study the proposed 20 kHz, A.C. power system. The

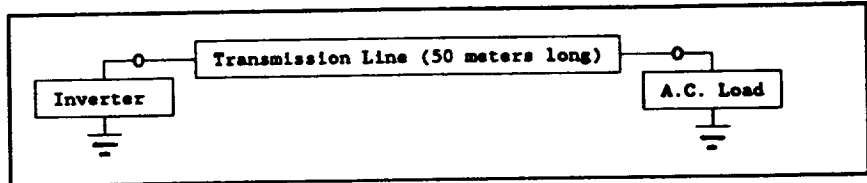


Figure 10 - General Dynamics Corporation (GDC) 20 kHz Testbed Power System.

inverter is a Mapham inverter set which will produce  $440 V_{rms}$  at 20 kHz. This inverter will have the following electrical characteristics:

$$L_r = 16 \mu H ,$$

$$C_r = 1.71 \mu F ,$$

$$C_s = 2.0 \mu F ,$$

$$L_1 = 1.8 \mu H ,$$

$$L_m = 1.0 mH , \text{ and}$$

$$f_s = 20 kHz .$$

The transmission line is a 50 meter length of stripline designed cable which has the following electrical characteristics:

$$Resistance = 1.043 \frac{m\Omega}{meter} ,$$

$$Inductance = 0.027 \frac{\mu H}{meter} , \text{ and}$$

$$Capacitance = 0.003 \frac{\mu F}{meter} .$$

The load is standard A.C. load which will be varied from 2 kVA to 10 kVA. The load will maintain a constant power factor of 80% lagging throughout this example. Figure 11 shows the data formatted for the harmonic power flow program. The load was varied from  $S = 0.16 + j 0.12$  p.u. to  $S = 0.80 + j 0.60$  p.u. The resulting Total Harmonic Distortion (THD) of the bus voltage, defined as

$$V_{THD} = \sum_{n=2}^{\infty} \frac{(V_i^{(n)})^2}{V_i^{(1)}} ,$$

was used to generate the graph shown in Figure 12. Note that the results of tests conducted by Sundberg, et. al. are also presented on the graph in Figure

```

1
NASA Test System
2
Test System for Paper #899383 of the IECEC '89 Conference, Vol. 1
3
1 Source1 08
16.0e-6 1.71e-6 2.0e-6 1.8e-6 0.0e-0 2.0e+4 100.00 0.0
3 Load1 03 24.0 18.0 440.0 1.0e+4
9999
4
1 3 0.54 1.75
1 0 0.0 -5305.
3 0 0.0 -5305.
3 0 266.7 200.0
1 0 0.0 649.09
9999
5
9 590 080 1 000 0
15

```

Figure 11 - Input Data from the GDC 20 kHz Testbed for the Harmonic Power Flow.

12. Examination of the graph in Figure 12 reveals that the harmonic power flow does yield results which are very close to the values obtained experimentally. It should also be noted that the results obtained from the harmonic power flow program are exceptionally sensitive to the impedance values. It was found that very small changes in the data will cause relatively large changes in the output.

The second example will also use the system described in Figure 10. This time the switching frequency will be varied to get the ratio  $f_r/f_s$  to vary from 0.6 to 0.95. The data for this example remains the same as that found in Figure 11 with the exception of the switching frequency. This value is varied as described above; and, the resulting THD of the bus voltage is compared to that measure by Sundberg, et. al. in Figure 13.

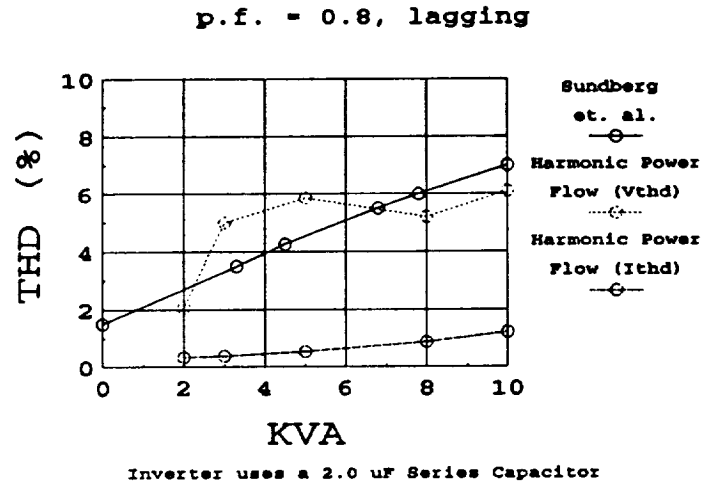


**Figure 12** - Comparison of Results of Bus Voltage THD versus KVA Loading from Harmonic Power Flow Program and Test Data from the GDC 20 kHz Testbed. Current THD versus KVA Loading is also included.

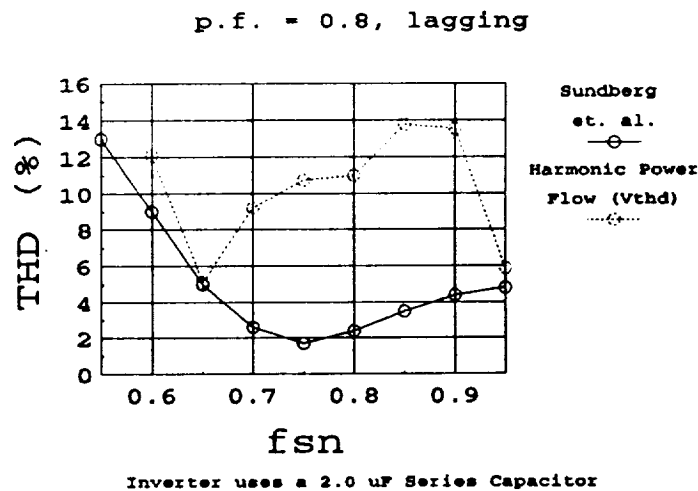


**Figure 13** - Comparison of Results of Bus Voltage THD versus  $f_{sn}$  from Harmonic Power Flow Program and Test Data from the GDC 20 kHz Testbed.



## **9. Conclusions and Recommendations**

This report for the 1990 Summer Faculty Fellowship Program documents the development of software which will benefit the design and analysis of large A.C. spacecraft power systems. Early results indicate that the models developed are quite adequate for the intended goals. This is demonstrated by the acceptable correlation of the results exhibited in Section 8. Although the results are not exact, the discrepancies are relatively small. Given the small discrepancies and the limited test results from the GDC 20 kHz Testbed for comparison, further comparisons are necessary before accurate conclusions concerning program accuracy can be drawn. Once the GDC 20 kHz Testbed is made operational in its new location, an organized set of tests should be devised which will thoroughly evaluate the models developed in this report. This evaluation will help refine the models.

As a result of the work cited in this report, the following areas are recommended for further investigation and development:

- complete voltage control for voltage controlled rectifier,
- model series and parallel operation of Mapham inverters, and
- model bidirectional receivers.

Implementation of the voltage controlled rectifier model discussed in Sections 4 and 5 was started during this time frame. The model, however, was not completed due to time constraints. The model, which is presently incorporated into the harmonic power flow program, is a single phase, full wave rectifier. The model for this device is exactly that of the single phase, voltage controlled rectifier with the exception that the voltage is determined by the system configuration and not controlled to a desired level. The work required to implement voltage control appears to be straightforward.

Mapham inverters are operated in series to increase the total output voltage of the source. The modelling of this operating configuration must be investigated so that this mode of operation can be included in future design reviews.

The bidirectional receiver unit is a device which is proposed for use on space vehicles. Modelling this device in the harmonic power flow program is important for a complete analysis of any proposed power system. For this reason, it is recommended that work be conducted in this area as well as those mentioned above.

## LIST OF REFERENCES

- [1] N. Mapham, "An SCR Inverter with Good Regulation and Sine-Wave Output," IEEE Trans. on Industry and General Applications, IGA-3, no. 2, pp. 176-187, March/April 1967.
- [2] A. S. Brush, R. C. Sundberg, R. M. Button, "Frequency Domain Model for Analysis of Paralleled, Series-Output-Connected Mapham Inverters," 24<sup>th</sup> Intersociety Energy Conversion Engineering Conference, Washington, D.C., August 1989.
- [3] R. C. Sundberg, A. S. Brush, R. M. Button, A. G. Patterson, "Distortion and Regulation Characterization of a Mapham Inverter," 24<sup>th</sup> Intersociety Energy Conversion Engineering Conference, Washington, D.C., August 1989.
- [4] D. Xia, G. T. Heydt, "Harmonic Power Flow Studies Part 1 - Formulation and Solution," IEEE Trans. on Power Apparatus and Systems, vol. PAS-101, no. 6, pp. 1257-65, June 1982.
- [5] D. Xia, G. T. Heydt, "Harmonic Power Flow Studies Part II - Implementation and Practical Applications," IEEE Trans. on Power Apparatus and Systems, vol. PAS-101, no. 6, pp. 1266-70, June 1982.
- [6] W. M. Grady, "Harmonic Power Flow Studies," Ph. D. Thesis, Purdue University, West LaFayette, IN, August 1983.
- [7] F. Williamson, G. B. Sheble, "Harmonic Analysis of Spacecraft Power Systems Using a Personal Computer," 24<sup>th</sup> IECEC, 1989.
- [8] R. Leskovich, I. G. Hansen, "The Effects of Nonlinear Loading Upon the Space Station Freedom 20 kHz Power System," 24<sup>th</sup> IECEC, August, 1989.

## Appendix A

### Derivation of Coefficients of System Responses

To find the polynomials of the input current it is simply a matter of employing Ohm's Law in the frequency domain,

$$I_{c_r}(s) = \frac{V_{in}(s)}{Z_{eq}(s)} .$$

When the Mapham inverter is connected to a power system which can be modelled as a series R-L circuit, the equivalent input impedance of the entire network is the impedance  $Z_{eq}$  shown in Figure A.1. The following steps are used to find  $Z_{eq}$  which is connected to the source.

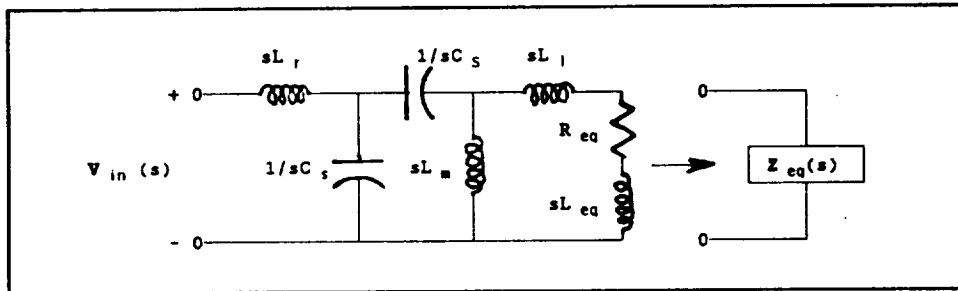


Figure A.1 - Total System Connected to the Source.

1. Series of  $sL_{eq}$ ,  $sL_{eq}$ , and  $R_{eq}$  yields  $Z_1(s)$ .

$$Z_1(s) = R_{eq} + s(L_1 + L_{eq}) .$$

2. Parallel of  $Z_1(s)$  and  $sL_m$  yields  $Z_2(s)$ .

$$\begin{aligned} Z_2(s) &= \frac{Z_1(s) (sL_m)}{Z_1(s) + sL_m} \\ &= \frac{s^2 L_m (L_1 + L_{eq}) + sR_{eq}L_m}{s(L_1 + L_{eq} + L_m) + R_{eq}} \end{aligned}$$

3. Series of  $Z_2(s)$  and  $1/sC_s$  yields  $Z_3(s)$ .

$$\begin{aligned} Z_3(s) &= \frac{1}{sC_s} + Z_2(s) \\ &= \frac{1}{sC_s} + \frac{s^2 L_m (L_1 + L_{eq}) + sR_{eq}L_m}{s(L_1 + L_{eq} + L_m) + R_{eq}} \\ &= \frac{s^3 C_s L_m (L_1 + L_{eq}) + s^2 R_{eq} L_m C_s + s(L_1 + L_{eq} + L_m) + R_{eq}}{s^2 C_s (L_1 + L_{eq} + L_m) + sR_{eq} C_s} \end{aligned}$$

4. Parallel of  $Z_3(s)$  and  $1/C_r$  yields  $Z_4(s)$ .

$$\begin{aligned} Z_4(s) &= \frac{\left( \frac{1}{sC_r} \right) Z_3(s)}{\frac{1}{sC_r} + Z_3(s)} \\ &= \frac{s^3 C_s L_m (L_1 + L_{eq}) + s^2 R_{eq} L_m C_s + s(L_1 + L_{eq} + L_m) + R_{eq}}{s^4 C_s C_r L_m (L_1 + L_{eq}) + s^3 R_{eq} L_m C_r C_s + s^2 C_s (L_1 + L_{eq} + L_m) + sR_{eq} (C_r + C_s)} \end{aligned}$$

5. Series  $Z_4(s)$  and  $sL_r$  yields  $Z_{eq}(s)$ .

$$Z_{eq}(s) = sL_r + Z_4(s)$$

$$= \frac{s^3 L_r L_m C_s C_r (L_1 + L_{eq}) + s^4 L_r L_m C_s C_r R_{eq} + s^3 [L_m C_s (L_1 + L_{eq}) + L_r (C_s + C_r) (L_1 + L_{eq} + L_m)] + s^2 (R_{eq} [L_r (C_s + C_r) + L_m C_s]) + s (L_1 + L_{eq} + L_m) + R_{eq}}{s^3 L_m C_s C_r (L_1 + L_{eq}) + s^4 L_m C_s C_r R_{eq} + s^3 [L_m C_s (L_1 + L_{eq}) + L_r (C_s + C_r) (L_1 + L_{eq} + L_m)] + s^2 (R_{eq} [L_r (C_s + C_r) + L_m C_s]) + s (L_1 + L_{eq} + L_m) + R_{eq}}$$

Since the Laplace transform of the switched input voltage is

$$\mathcal{L}[V_m u(t)] = \frac{1}{s},$$

then the input current is

$$I_{c_s}(s) = \frac{\frac{1}{s}}{Z_{eq}}(s)$$

$$= \frac{s^3 L_m C_s C_r (L_1 + L_{eq}) + s^4 L_m C_s C_r R_{eq} + s [(C_s + C_r) (L_1 + L_{eq} + L_m)] + R_{eq} (C_s + C_r)}{s^3 L_m C_s C_r (L_1 + L_{eq}) + s^4 L_m C_s C_r R_{eq} + s^3 [L_m C_s (L_1 + L_{eq}) + L_r (C_s + C_r) (L_1 + L_{eq} + L_m)] + s^2 (R_{eq} [L_r (C_s + C_r) + L_m C_s]) + s (L_1 + L_{eq} + L_m) + R_{eq}}$$

The denominator of the above equation yields the coefficients which are necessary to find the natural response of the input current.

When the power system equivalent is a series R-C circuit rather than the series R-L which is shown above, the method outlined above is used to find the coefficients of the polynomial in the denominator of the current's function in the frequency domain.



# REPORT DOCUMENTATION PAGE

Form Approved  
OMB No. 0704-0188

Public reporting burden for this collection of information is estimated to average 1 hour per response, including the time for reviewing instructions, searching existing data sources, gathering and maintaining the data needed, and completing and reviewing the collection of information. Send comments regarding this burden estimate or any other aspect of this collection of information, including suggestions for reducing this burden, to Washington Headquarters Services, Directorate for Information Operations and Reports, 1215 Jefferson Davis Highway, Suite 1204, Arlington, VA 22202-4302, and to the Office of Management and Budget, Paperwork Reduction Project (0704-0188), Washington, DC 20503.

1. AGENCY USE ONLY (Leave blank)		2. REPORT DATE November 1991	3. REPORT TYPE AND DATES COVERED Technical Memorandum	
4. TITLE AND SUBTITLE Development of a Single-Phase Harmonic Power Flow Program to Study the 20 kHz A.C. Power System for Large Spacecraft			5. FUNDING NUMBERS  WU-506-41-41	
6. AUTHOR(S) L. Alan Kraft and M. David Kankam				
7. PERFORMING ORGANIZATION NAME(S) AND ADDRESS(ES) National Aeronautics and Space Administration Lewis Research Center Cleveland, Ohio 44135-3191			8. PERFORMING ORGANIZATION REPORT NUMBER  E-6687	
9. SPONSORING/MONITORING AGENCY NAMES(S) AND ADDRESS(ES) National Aeronautics and Space Administration Washington, D.C. 20546-0001			10. SPONSORING/MONITORING AGENCY REPORT NUMBER  NASA TM-105326	
11. SUPPLEMENTARY NOTES L. Alan Kraft, Valparaiso University, Valparaiso, Indiana 46383 and NASA/ASEE Summer Faculty Fellow at Lewis Research Center in 1990. M. David Kankam, NASA Lewis Research Center. Responsible person, M. David Kankam, (216) 433-6143.				
12a. DISTRIBUTION/AVAILABILITY STATEMENT  Unclassified - Unlimited Subject Category 20			12b. DISTRIBUTION CODE	
13. ABSTRACT (Maximum 200 words)  This report describes the development of a software to aid in the design and analysis of AC power systems for large spacecraft. The algorithm is an improved version of Electric Power Research Institute's (EPRI) harmonic power flow program, "HARMFLO", used for the study of AC power quality. The new program is applicable to three-phase systems typified by terrestrial power systems, and single-phase systems characteristic of space power systems. The modified "HARMFLO" accommodates system operating frequencies ranging from terrestrial 60 hz to and beyond aerospace 20 kHz, and can handle both source and load-end harmonic distortions. Comparison of simulation and test results of a representative spacecraft power system shows a satisfactory correlation. Recommendations are made for the direction of future improvements to the software, to enhance its usefulness to power system designers and analysts.				
14. SUBJECT TERMS Space power systems; Harmonic power flow; Power systems analysis			15. NUMBER OF PAGES 36	
			16. PRICE CODE A03	
17. SECURITY CLASSIFICATION OF REPORT Unclassified	18. SECURITY CLASSIFICATION OF THIS PAGE Unclassified	19. SECURITY CLASSIFICATION OF ABSTRACT Unclassified	20. LIMITATION OF ABSTRACT	